

# EZH2-specific microRNA-98 inhibits human ovarian cancer stem cell proliferation via regulating the pRb-E2F pathway

Te Liu · Lengchen Hou · Yongyi Huang

Received: 21 February 2014 / Accepted: 6 April 2014 / Published online: 27 April 2014  
© International Society of Oncology and BioMarkers (ISOBM) 2014

**Abstract** The Polycomb group protein, enhancer of zeste homolog 2 (EZH2), plays an important role in transcriptional regulation through chromatin remodeling and interactions with other transcription factors to control cell proliferation and embryonic development. Previous study has shown that EZH2 is important for cell cycle regulation and is highly expressed in human ovarian cancer. Loss of EZH2 inhibits growth of ovarian cancer as well as other human carcinomas. In this study, an expression plasmid of EZH2-targeted microRNA-98 was constructed and transfected into human ovarian cancer stem cells (OCSCs). Seventy-two hours after transfection, cell growth was inhibited and arrested at the G<sub>0</sub>/G<sub>1</sub> transition. p21<sup>CIP1/WAF1</sup> was up-regulated, while the CDK2/cyclin E complex and c-Myc were down-regulated. Most importantly, expression levels of E2F1, retinoblastoma protein (pRb), and histone deacetylase 1 (HDAC1) in the pRb–E2F signaling pathway had changed. Furthermore, microRNA-98 suppressed the growth of OCSCs xenograft tumors. Our findings suggest that EZH2-specific microRNA-98 can effectively inhibit cell proliferation in vitro and regulate the pRb–E2F pathway in human OCSCs.

**Keywords** Ovarian cancer stem cells · EZH2 · MicroRNA-98 · pRb-E2F pathway · Cell proliferation

T. Liu (✉) · L. Hou  
Shanghai Tenth People's Hospital, Medical School,  
Tongji University, Shanghai 200072, China  
e-mail: liutelt@163.com

T. Liu  
Shanghai Geriatric Institute of Chinese Medicine, Longhua Hospital,  
Shanghai University of Traditional Chinese Medicine,  
Shanghai 200031, China

Y. Huang  
Laboratoire PROTEE, Bâtiment R, Université du Sud Toulon-Var,  
83957 La Garde Cedex, France

## Introduction

In 2008 and 2010, CD44<sup>+</sup>/CD117<sup>+</sup> ovarian cancer stem cells (OCSCs) were isolated and enriched from human primary ovarian tumor tissues and confirmed by flow cytometry sorting by Zhang et al. [1] and Liu et al. [2]. Most ovarian cancer patients receive chemotherapy throughout the course of their long-term treatment; it is a common and conservative treatment for ovarian cancer. Despite this treatment, cancer cells still invade and metastasize in many patients [2–4]. Several studies indicate that OCSCs are the root of metastasis and invasion in ovarian cancer [2–4]; however, the mechanisms responsible for the development of highly proliferative and invasive OCSCs are complicated and thus far poorly understood. Proteins encoded by the Polycomb-group (PcG) family of genes are known to play crucial roles in the gene expression program that allows stem cells to maintain a pluripotent state, being able to differentiate into specialized phenotypes when signaled to do so. PcG proteins were first described in *Drosophila* where they were shown to repress the homeotic genes that control segment identity in the developing embryo [5–9]. The enhancer of zeste homolog 2 (EZH2) gene is a human homolog of the *Drosophila* PcG gene, enhancer of Zest [E(z)] [10]. EZH2 is a component of the Polycomb repressive complex 2 (PRC2), which along with embryonic ectoderm development (EED) and suppressor of zeste (Su(z)12), initiates stable transcriptional repression in early embryogenesis [11, 12]. PRC1 subsequently maintains transcriptional silencing. EZH2 contains a highly conserved, C-terminal SET (Su(var)3-9, enhancer of zeste, and Trithorax) domain that catalyzes the addition of methyl groups to histone H3 at lysines 27 and 9, with a strong preference for methylating K27 [10, 11, 13, 14]. One of the earliest reports of EZH2 was from a gene profiling study where EZH2 was identified as the most significantly overexpressed gene in metastatic prostate cancer. The study also showed that loss of EZH2 inhibited

growth of OCSCs [15–17]. Similar requirements for EZH2 in the proliferation of other cell types have been described [15–17]. Analysis of patient samples has also shown that elevated EZH2 levels significantly correlate with invasiveness and increased proliferation rates of breast carcinomas [18, 19]. MicroRNAs (miRNAs) are small RNA molecules (21–23 nt) that act as negative regulators of gene expression, either by blocking mRNA translation or through RNA interference [3, 4, 20–23]. Previous studies revealed that dysregulation of specific miRNAs were associated with certain types of OCSCs; these specific miRNAs act as either oncogenes or tumor suppressors, depending on the target gene [3, 4]. In this study, EZH2-targeted microRNA-98 was constructed and applied to transfect a human OCSCs line, 22RV1. We found the growth of these transfected cells were inhibited and arrested at the G<sub>0</sub>/G<sub>1</sub> transition. In addition, p21<sup>CIP1/WAF1</sup> was up-regulated, while the CDK2/cyclin E complex and c-Myc were down-regulated. Expression levels of E2F1, retinoblastoma protein (pRb), and histone deacetylase (HDAC1) of the pRb–E2F signaling pathway altered. Our results demonstrated that EZH2-specific microRNA-98 effectively inhibits human OCSCs proliferation in vitro and regulates the pRb–E2F pathway.

## Materials and methods

### Isolation of CD44<sup>+</sup>/CD117<sup>+</sup> ovarian tumor cells by fluorescence-activated cell sorting

Ovarian tumors were collected from the inpatient clinic of Shanghai Tenth People's Hospital (Shanghai, China) between May 2013 and Dec 2013. CD44<sup>+</sup>/CD117<sup>+</sup> cell subpopulations were isolated from tumor samples, as previously described [1–4]. Briefly, 4 μl each of 10 mg/ml mouse anti-human CD117-FITC and rabbit anti-human CD44-PE (eBioscience) in a final volume of 1.0 ml were added to sedimented cells and incubated at 4 °C in phosphate buffered saline (PBS) for 30 min to block nonspecific binding. Cells were then washed twice in PBS and CD44<sup>+</sup>/CD117<sup>+</sup> cells were isolated by flow cytometry (BD FACSAria; BD Bioscience, San Jose, CA, USA), incubated at 10 °C in PBS for 15 min and then washed twice in PBS. Isolated CD44<sup>+</sup>/CD117<sup>+</sup> OCSCs were plated at 1,000 cells/ml in DMEM:F12 medium (HyClone), supplemented with 10 ng/ml bFGF, 10 ng/ml EGF, 5 μg/ml insulin and 0.5 % BSA (all obtained from Sigma-Aldrich, St. Louis, MO, USA) and grown at 37 °C in a humidified atmosphere containing 5 % CO<sub>2</sub>. The resulting nonadherent spherical OCSC clusters were grown until passage 4 before being used for experiments.

### Reporter vector construction

A microRNA expression reporter plasmid was constructed as previously described [3, 4]. A negative control plasmid was

constructed similarly, except that 11 nucleotides in the miRNA-98 seed sequence were mutated (GAGGTAGTAAGTGTATTGT was changed to GtGcTtGTtAcaTcaActGT; mutations in lower case). OCSCs were transfected with 0.3 μg wild-type (WT) or mutant (Mut) miRNA-98 vector using Lipofectamine 2000 (Invitrogen), according to the manufacturer's protocol.

### Luciferase report assay

Luciferase report assays were done as previously described [3, 4]. NIH-3T3 mouse embryonic fibroblast cells were seeded at 3 × 10<sup>4</sup>/well in 48-well plates and co-transfected with 400 ng pRNAT-CMV32-mir98-WT, pRNAT-CMV32-mir98-Mut or pRNAT-CMV32 (empty vector); 20 ng pGL3-EZH2-3UTR-WT or pGL3-EZH2-3UTR-Mut; and pRL-TK (Promega, Madison, WI, USA) using Lipofectamine 2000 according to the manufacturer's protocol. Luciferase activity was measured after 48 h using the Dual-Luciferase Reporter Assay System (Promega).

### Northern blotting

Northern blotting was done as previously described [3, 4]. For all cell treatment groups, 20 μg of good-quality total RNA was analyzed on a 7.5 M urea, 12 % PAA denaturing gel and transferred to a Hybond N<sup>+</sup> nylon membrane (Amersham, Freiburg, Germany). Membranes were cross-linked using ultraviolet light for 30 s at 1,200 mJ/cm<sup>2</sup> and hybridized to the miRNA-98 antisense Starfire probe, 5'-AAGAATACAAC TACTACCTCA-3' (IDT, Coralville, IA, USA) for the detection of 22-nt miRNA-98 fragments, according to the manufacturer's instructions. After washing, membranes were exposed to Kodak XAR-5 film for 20–40 h (Sigma-Aldrich). A human U6 snRNA probe (5'-GCAGGGGCCATGCTAATC TTCTCTGTATCG-3') was used as a positive control, with an exposure time of 15–30 min.

### Methyl thiazolyl tetrazolium (MTT) assay for cell proliferation

Cells were seeded at 2 × 10<sup>3</sup> per well in 96-well plates and cultured in DMEM:F12 supplemented with 10 % FBS at 37 °C with 5%CO<sub>2</sub>, until 85 % confluent. MTT (Sigma) reagent (5 mg/ml) was added to the maintenance cell medium at different time points, and incubated at 37 °C for an additional 4 h. The reaction was terminated with 150 μl dimethylsulfoxide (DMSO; Sigma) per well and the cells were lysed for 15 min, and the plates were gently shaken every 5 min. Absorbance values were determined by using the enzyme linked immunosorbent assay (ELISA) reader (Model 680; Bio-Rad) at 490 nm.

### Flow cytometric (FCM) analysis of cell cycle by propidium iodide (PI) staining

Cells were washed three times by PBS and then were collected by centrifugation (Allegra X-22R; Beckman Coulter) at  $1,000\times g$  for 5 min. The cell pellets were resuspended in 1 ml of PBS, fixed in 70 % ice-cold ethanol, and kept in a freezer for more than 48 h. Before FCM analysis, the fixed cells were centrifuged, washed twice with PBS, and resuspended in PI staining solution (Sigma) containing 50  $\mu\text{l/ml}$  PI and 250  $\mu\text{g/ml}$  RNase A (Sigma). The cell suspension, which was hidden from light, was incubated for 30 min at 4 °C and analyzed using the FACS (FCM-500, Beckman Coulter). A total of 10,000 events were acquired for analysis using CellQuest software.

### Quantitative real-time PCR (qRT-PCR) analysis

Cells were seeded at  $3\times 10^5$  per well in 6-well plates and cultured for 72 h before being transfected. Total RNAs from each treatment group were isolated using Trizol Reagent according to the manufacturer's protocol. The RNA samples were treated with DNase I (Sigma), quantified, and reverse-transcribed into cDNA using the ReverTra Ace- $\alpha$  First Strand cDNA Synthesis Kit. qRT-PCR was conducted using a RealPlex4 real-time PCR detection system from Eppendorf Co. Ltd (Germany), with SyBR Green RealTime PCR Master MIX used as the detection dye. qRT-PCR amplification was performed over 40 cycles with denaturation at 95 °C for 15 s and annealing at 58 °C for 45 s. Target cDNA was quantified using the relative quantification method. A comparative threshold cycle ( $C_t$ ) was used to determine gene expression relative to a control (calibrator) and steady-state mRNA levels are reported as  $n$ -fold difference relative to the calibrator. For each sample, the EZH2 and cGFP  $C_t$  values were normalized using the formula  $\Delta C_t = C_{t\_EZH2} - C_{t\_18sRNA}$ . To determine relative expression levels, the following formula was used  $\Delta\Delta C_t = \Delta C_{t\_sample} - \Delta C_{t\_calibrator}$ . The values used to plot relative EZH2 or cGFP expression were calculated using the expression  $2^{-\Delta\Delta C_t}$ . The mRNA levels were calibrated based on levels of 18 s RNA (24).

### Co-immunoprecipitation (Co-IP) assay

Each group cells were seeded at  $3\times 10^5$  per well in 6-well plates and cultured until 85 % confluent, which were lysed (500  $\mu\text{l/plate}$ ) in a modified cell lysis buffer for Western and IP (20 mM Tris, pH 7.5, 150 mM NaCl, 1 % Triton X-100, 1 mM EDTA, sodium pyrophosphate,  $\beta$ -glycerophosphate,  $\text{Na}_3\text{VO}_4$  and leupeptin) (Beyotime Institute of Biotechnology). After lysis, each sample was centrifuged to clear the lysate of the insoluble debris and preincubated with 20  $\mu\text{g}$  protein A agarose beads (Beyotime Institute of

Biotechnology) by rocking for 30 min at 4 °C, followed by centrifugation and transfer to a fresh 1.5-ml tube. The primary antibody was incubated for 90 min before re-addition of 20  $\mu\text{g}$  protein A agarose beads to capture the immune complexes (Table 1). The pelleted beads were then washed three times with 500  $\mu\text{l}$  cell lysis buffer, dissolved in 4 $\times$  SDS-PAGE samples loading buffer, and heated for 10 min at 95 °C.

### Western blotting analysis

Protein products of each group were dissolved in 4 $\times$  SDS-PAGE samples loading buffer, and heated for 10 min at 95 °C after being quantified by the method of Lowry et al. The proteins were resolved by 12 % SDS-PAGE, transferred on PVDF (Millipore) membranes and then, the PVDF membranes were blocked by 5 % BSA (Sigma) in TBST (20 mM Tris, 150 mM NaCl, 0.2 % Tween-20, pH 7.6) at 4 °C overnight. After blocking, the PVDF membranes were washed four times for 15 min with TBST at room temperature, and incubated for 1 h with primary antibodies (Table 1). Following extensive washing with TBST, the PVDF membranes were incubated for 1 h with appropriate secondary antibody. Finally, the PVDF membranes were washed four times for 15 min with TBST at room temperature. Following washing, the PVDF membranes were incubated in enhanced chemiluminescent Western blotting detection system kit (Pierce Biotechnology, Rockford, IL, USA), and exposed to X-ray films (Kodak).

### In vivo xenograft experiments

Approximately  $1\times 10^4$  logarithmically growing OCSCs were inoculated into BALB/c nude mice. Each experimental group consisted of three mice. After 12 weeks, mice were sacrificed and tumors were excised. Tumor weight was measured and tumor volume was calculated according to this formula: Tumor volume ( $\text{mm}^3$ ) =  $(ab^2)/2$ , where  $a$  is the longest axis (mm) and  $b$  is the shortest axis (mm).

### Statistical analysis

Each experiment was performed as least three times, and data were shown as the mean  $\pm$  SE where applicable, and differences were evaluated using Mann–Whitney test. The probability of  $<0.05$  was considered statistically significant.

## Results

### Patient population

A total of six ovarian cancer patients were included in this study. The characteristics of all ovarian patients are summarized in Table 2. The age, stage, grade of differentiation, and

**Table 1** Primary antibodies list

Antibodies	Manufacturer	Applications
Rabbit anti-human E2F1	Cell Signaling Technology, Danvers, MA, USA	WB (1:1,000)
Rabbit anti-human EZH2	Cell Signaling Technology, Danvers, MA, USA	WB (1:1,000)
Rabbit anti-human p21	Cell Signaling Technology, Danvers, MA, USA	WB (1:1,000)
Rabbit anti-human cyclin E	Cell Signaling Technology, Danvers, MA, USA	WB (1:1,000)
Rabbit anti-human c-Myc	Cell Signaling Technology, Danvers, MA, USA	WB (1:1,000)
Rabbit anti-human pRB	Cell Signaling Technology, Danvers, MA, USA	WB (1:1,000)
Rabbit anti-human HDAC1	Cell Signaling Technology, Danvers, MA, USA	WB (1:1,000)
Rabbit anti-human CDK2	Cell Signaling Technology, Danvers, MA, USA	WB (1:1,000)
Rabbit anti-GAPDH	Cell Signaling Technology, Danvers, MA, USA	WB (1:1,000)

histology distribution of these patients is based on the International Federation of Gynecology and Obstetrics (FIGO) annual report for European countries.

#### Identification of miRNA-98 binding sites in the EZH2 3' UTR

The miRBase Target database was used to analyze precursor miRNA (pre-miRNA) sequences, mature miRNA sequences,

**Table 2** Characteristics of the patients' cohort

	Patients ( <i>n</i> =6)
Age median (range), years	28–61
≤40	2
40–60	3
≥60	1
Surgical staging	
Ia, Ib, Ic	1
IIa, IIb, IIc	3
IIIa, IIIb, IIc	2
IV	–
Histopathology	
Serous	2
Endometrioid	1
Mucinous	1
Clear cells	1
Others (mixed epithelial, undifferentiated)	1
Tumor grade	
1	1
2	3
3 or clear cell	2
Unknown	–
Treatments	
Primary surgery	3
Radical surgery	–
Secondary surgery	–
Platinum-based chemotherapy	3
Radiotherapy	–

chromosomal locations, the length of miRNA-98, and potential target sites in the *EZH2* gene. A putative 7-nt miRNA target site was identified in the *EZH2* mRNA 3' untranslated region (3' UTR) of several mammalian species (Fig. 1). To examine whether *EZH2* expression is regulated by mature miRNA-98, a luciferase reporter containing a WT or Mut *EZH2* 3' UTR miRNA-98 binding site, or an empty plasmid control, was co-transfected with miRNA-98 expression vectors (WT-miRNA-98, Mut-miRNA-98 or empty vector control) into NIH-3T3 cells. The activity of the luciferase reporter containing WT *EZH2* 3' UTR was significantly inhibited by miRNA-98 cotransfection, while the activity of the reporter containing the mutated *EZH2* 3' UTR site was unaffected by miRNA-98 cotransfection (Fig. 1). These results demonstrate that miRNA-98 targets *EZH2* mRNA by specifically binding to the 3' UTR.

#### Mature miRNA-98 downregulation in CD44<sup>+</sup>/CD117<sup>+</sup> OCSCs correlates with *EZH2* overexpression

The qRT-PCR result showed that *EZH2* mRNA expression was significantly higher in OCSCs than in CD44<sup>−</sup>/CD117<sup>−</sup> ovarian cancer cells (OCCs) (Fig. 1). Moreover, the result of Northern blotting indicated that miRNA-98 hybridization signals were weaker in OCSCs extracts than in OCCs extracts, thus revealing that miRNA-98 is downregulated in OCSCs (Fig. 1). In addition, qRT-PCR analysis demonstrated that *EZH2* mRNA expression is reduced following miRNA-98 transfection in OCSCs, in contrast to cells transfected with Mut miRNA-98 (Fig. 1). However, the expression level of miRNA-98 in miRNA-98-transfected OCSCs was elevated of the time course, compare to it in untransfected group and miRNA-Mut transfected group (Fig. 1). These data show an inverse correlation between miRNA-98 and *EZH2* expression.

#### Proliferation of OCSCs is inhibited by miRNA-98 mediated *EZH2* gene silencing

The results of the proliferation assays performed are shown in Fig. 2. Using an MTT assay, the inhibition rate of miRNA-98

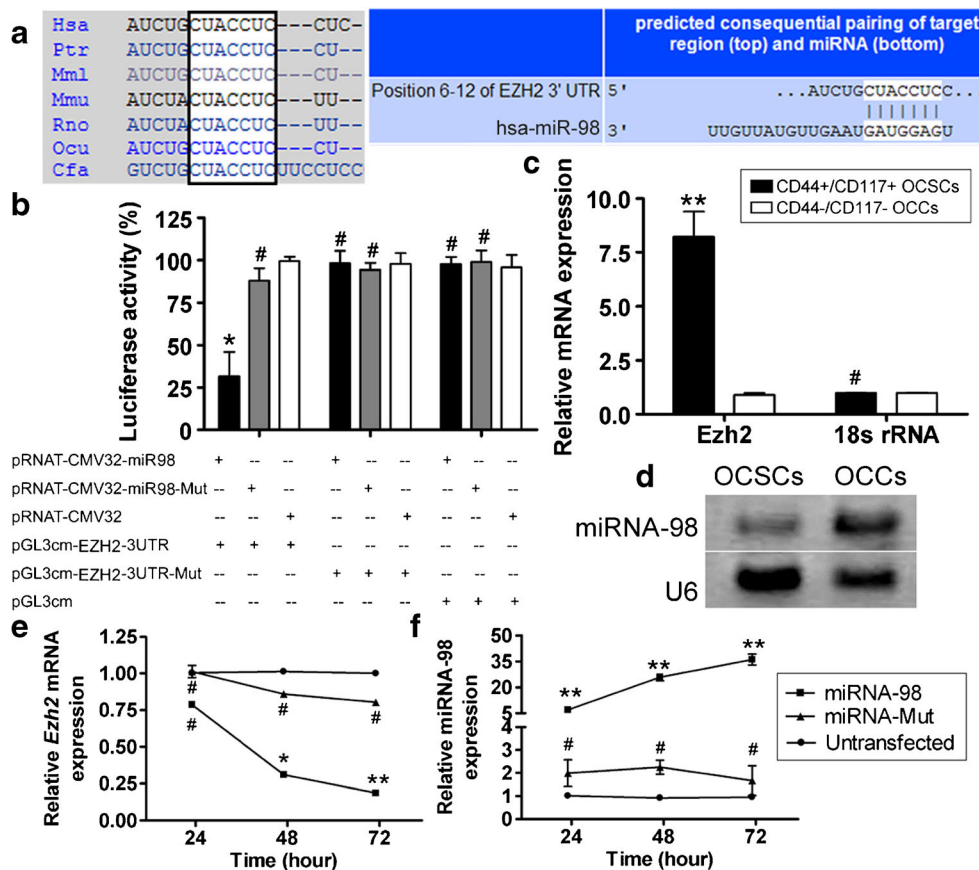


**Fig. 1** *EZH2* is a specific miRNA-98 target. **a** The mature miRNA-98 sequence was 100 % homologous in all species examined. Complementarity between miRNA-98 and the human *EZH2* 3' UTR target site is shown. **b** Luciferase reporter assays in NIH-3T3 mouse embryonic fibroblast cells. Plasmid DNA containing the *EZH2* 3' UTR miRNA-98-binding site (pGL3cm-*EZH2*-3UTR-WT), mutated *EZH2* 3' UTR miRNA-98-binding site (pGL3cm-*EZH2*-3UTR-Mut) or empty plasmid (pGL3cm) were cotransfected with an miRNA-98 expression vector (WT, Mut, or empty vector). Activity of the reporter containing the *EZH2* 3' UTR was specifically inhibited by miRNA-98 coexpression ( $*P < 0.05$  vs. pGL3cm transfection;  $^{\#}P > 0.05$  vs. pGL3cm transfection;  $n = 6$ ). **c** qRT-PCR analysis of *Ezh2* mRNA expression in OCSCs and OCCs. Relative

mRNA expression was normalized to 18S rRNA ( $**P < 0.01$  vs. OCCs;  $^{\#}P > 0.05$  vs. OCCs;  $n = 6$ ). **d** Northern blot of endogenous miRNA-98 expression in OCSCs and OCCs. U6 snRNA was used as a loading control. **e** qRT-PCR analysis of *EZH2* mRNA expression in miRNA-98 transfected OCSCs, miRNA-Mut transfected OCSCs or untransfected group on each time point. Relative mRNA expression was normalized to that of 18S rRNA ( $**P < 0.01$  vs. untransfected;  $*P < 0.05$  vs. untransfected;  $^{\#}P > 0.05$  vs. untransfected;  $n = 6$ ). **f** microRNA-qRT-PCR analysis of miRNA-98 expression in miRNA-98 transfected OCSCs, miRNA-Mut transfected OCSCs or untransfected group on each time point. Relative mRNA expression was normalized to that of U6 snRNA ( $**P < 0.01$  vs. untransfected;  $^{\#}P > 0.05$  vs. untransfected;  $n = 6$ )

transfected cells was shown to be markedly higher than non-transfected cells or miRNA-mut transfected cells at both 48 h and 72 h post-transfection (Table 3). In contrast, the viability of each group cells did not show any differences in proliferation at 24 h. But the inhibition rates remained unchanged for untransfected cells and miRNA-98-Mut transfected cells for the remainder of the time course. These data indicate that inhibition of *EZH2* expression reduces the viability of OCSCs in vitro.

#### Cell cycle changes induced by miRNA-98 expressing

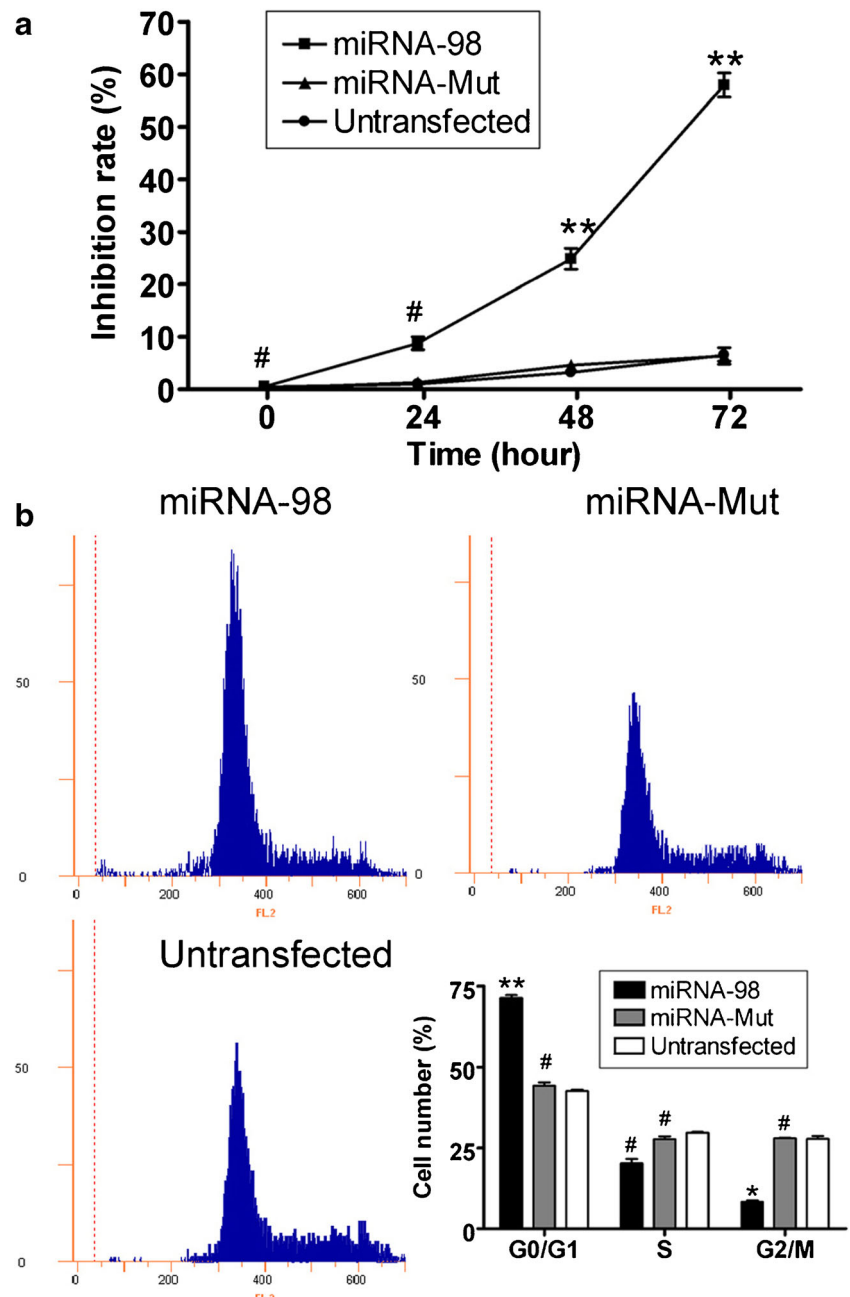
To detect changes in cell cycle progression for OCSCs, each group cells were stained with PI and analyzed by flow cytometry. The results showed that most of the miRNA-98 transfected cells were arrested in the  $G_0/G_1$  phase of the cell

cycle and the percentage of cells in  $G_2/M$  phase were markedly decreased. In contrast, there were no significant differences in the cell cycle distribution of the miRNA-98-Mut transfected and untransfected cells (Fig. 2). These cell cycle results suggest that knockdown of *EZH2* expression affects cell cycle regulation by miRNA-98.

#### The effects of miRNA-98 on the pRB-E2F pathway

First, the results of qRT-PCR showed that the levels of *Hdac1*, *E2f1*, *Ccne*, *Cdk2* and *pRb* mRNAs were significantly lower in OCSCs transfected with miR-98 expressing plasmids than in those transfected with mutant miR-98 plasmids or untransfected group. Conversely, the levels of *p21* mRNA was significantly higher in the miR-98-transfected cells (Fig. 3). co-IP and Western blot analysis were used to evaluate

**Fig. 2** miRNA-98 overexpression inhibits the proliferation capacity and cell cycle of OCSCs. **a** MTT assays of each group (\*\* $P < 0.01$  vs. untransfected; # $P > 0.05$  vs. untransfected;  $n = 6$ ). **b** Flow cytometry analysis showed that the majority of the miRNA-98 transfected OCSCs were arrested in the G0/G1 phase of the cell cycle and the percentage of cells in the G2/M phases was markedly decreased (\*\* $P < 0.01$  vs. untransfected; \* $P < 0.05$  vs. untransfected; # $P > 0.05$  vs. untransfected;  $n = 6$ )



the relative expression of the PcG proteins, as well as proteins upstream and downstream of the PcG proteins. As shown in Fig. 3, levels of EZH2, E2F1 and HDAC1 decreased in

OCSCs transfected with miRNA-98 ( $0.400 \pm 0.070$ ,  $0.325 \pm 0.025$  and  $0.100 \pm 0.020$ , respectively). These changes in above proteins were significant relative to miRNA-Mut

**Table 3** The MTT results of cell proliferation inhibition rate

Time (h)	miRNA-98 transfected OCSCs ( $n = 6$ )	miRNA-Mut transfected OCSCs ( $n = 6$ )	Untransfected OCSCs ( $n = 6$ )
0	0.54 ± 0.18 %	0.26 ± 0.12 %	0.52 ± 0.21 %
24	8.79 ± 2.12 %	1.29 ± 1.03 %	1.02 ± 0.77 %
48	24.88 ± 3.42 %	4.62 ± 1.17 %	3.25 ± 1.15 %
72	57.97 ± 4.01 %	6.38 ± 2.73 %	6.54 ± 1.92 %

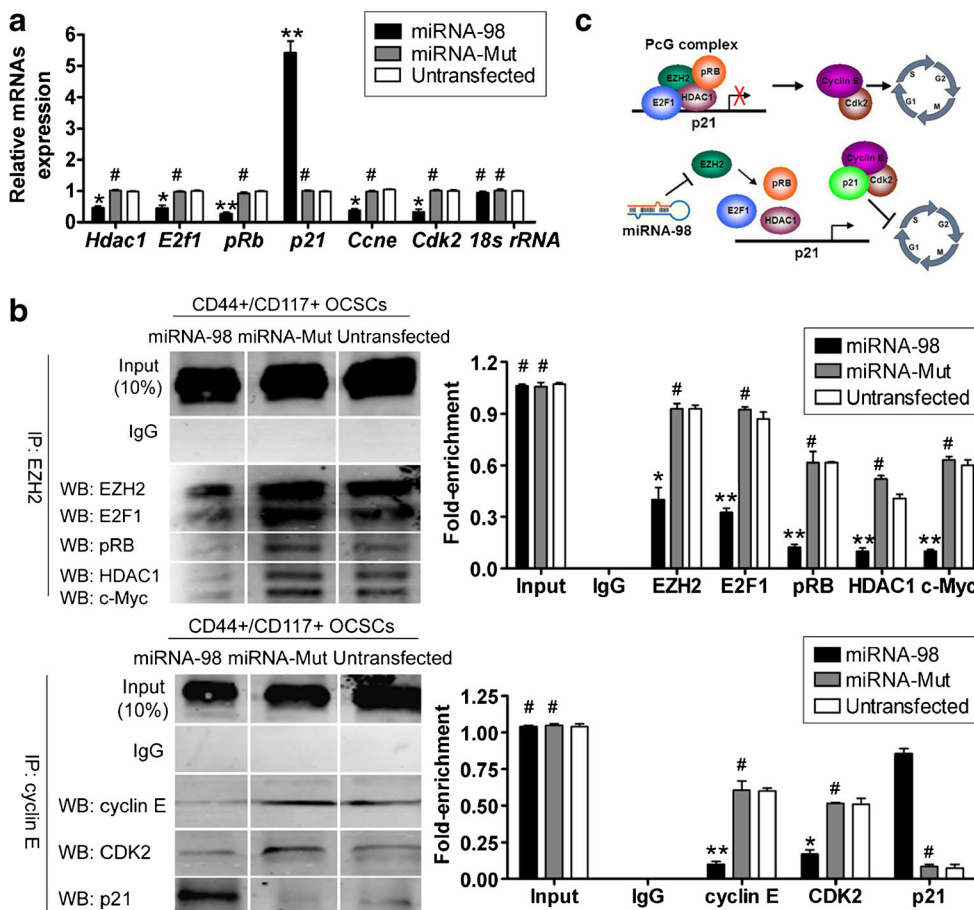


**Fig. 3** miRNA-98 regulates the PcG proteins and cell cycle factors expression. **a** The results of qRT-PCR showed that the levels of *Hdac1*, *E2f1*, *Ccne*, *Cdk2* and *pRb* mRNAs were significantly lower in miRNA-98 transfected OCSCs than them in miRNA-Mut transfected OCSCs or untransfected group. Conversely, the levels of *p21* mRNA was significantly higher in miRNA-98 transfected OCSCs. Relative mRNA expression was normalized to that of 18S rRNA (\*\**P*<0.01 vs. untransfected; \**P*<0.05 vs. untransfected; #*P*>0.05 vs. untransfected; *n*=6). **b** Co-immunoprecipitation (*co-IP*) and Western blot analysis indicated that levels of EZH2, E2F1 and HDAC1 decreased in miRNA-98 transfected

OCSCs. Meanwhile, the expression of pRB and c-Myc decreased in miRNA-98 transfected cells relative to miRNA-Mut and untransfected cells. Moreover, expression of cyclin E and CDK2 expressed at lower levels in miRNA-98 transfected OCSCs. However, the expression of p21 in miRNA-98 transfected cells was higher than in miRNA-Mut and untransfected cells. Then, for all proteins evaluated, there was no significant difference in protein levels between miRNA-Mut transfected cells and untransfected cells (\*\**P*<0.01 vs. untransfected; \**P*<0.05 vs. untransfected; #*P*>0.05 vs. untransfected; *n*=6). **c** The process of miRNA-98 regulated the PcG proteins and cell cycle

( $0.930\pm 0.030$ ,  $0.925\pm 0.015$  and  $0.520\pm 0.020$ , respectively) and untransfected cells ( $0.930\pm 0.020$ ,  $0.870\pm 0.040$  and  $0.405\pm 0.025$ , respectively). Meanwhile, the expression of pRB and c-Myc decreased in miRNA-98 transfected cells ( $0.125\pm 0.015$  and  $0.101\pm 0.012$ , respectively) relative to miRNA-Mut ( $0.615\pm 0.065$  and  $0.631\pm 0.021$ , respectively) and untransfected cells ( $0.615\pm 0.005$  and  $0.602\pm 0.031$ , respectively). In addition, expression of cyclin E and CDK2 were detected and were found to be expressed at lower levels in miRNA-98 cells ( $0.103\pm 0.021$  and  $0.172\pm 0.031$ , respectively) than in miRNA-Mut ( $0.605\pm 0.065$  and  $0.515\pm 0.005$ , respectively) or untransfected ( $0.603\pm 0.021$  and  $0.512\pm 0.041$ , respectively) cells. In contrast, the expression of p21 in miRNA-98 transfected cells ( $0.855\pm 0.035$ ) was higher than in miRNA-Mut ( $0.085\pm 0.015$ ) and untransfected cells ( $0.075\pm 0.025$ ). However, for all proteins evaluated, there was no

significant difference in protein levels between miRNA-Mut transfected cells and untransfected cells. The results based on co-IP and Western blot analyses suggested that EZH2 regulated the PcG proteins, HDAC1, E2F1, and pRb, yet also had the potential to affect the expression of additional proteins both upstream and downstream.

miR-98 overexpression inhibits OCSCs xenograft growth

The effect of miR-98 overexpression on tumor growth in vivo was investigated by subcutaneous inoculation of miR-98 or Mut-transfected OCSCs into nude mice. The tumors were analyzed after the mice were sacrificed 8 weeks following inoculation. As shown in Fig. 4, the tumor volume was substantially reduced by miR-98 overexpression. Although mice in both groups eventually developed tumors, those

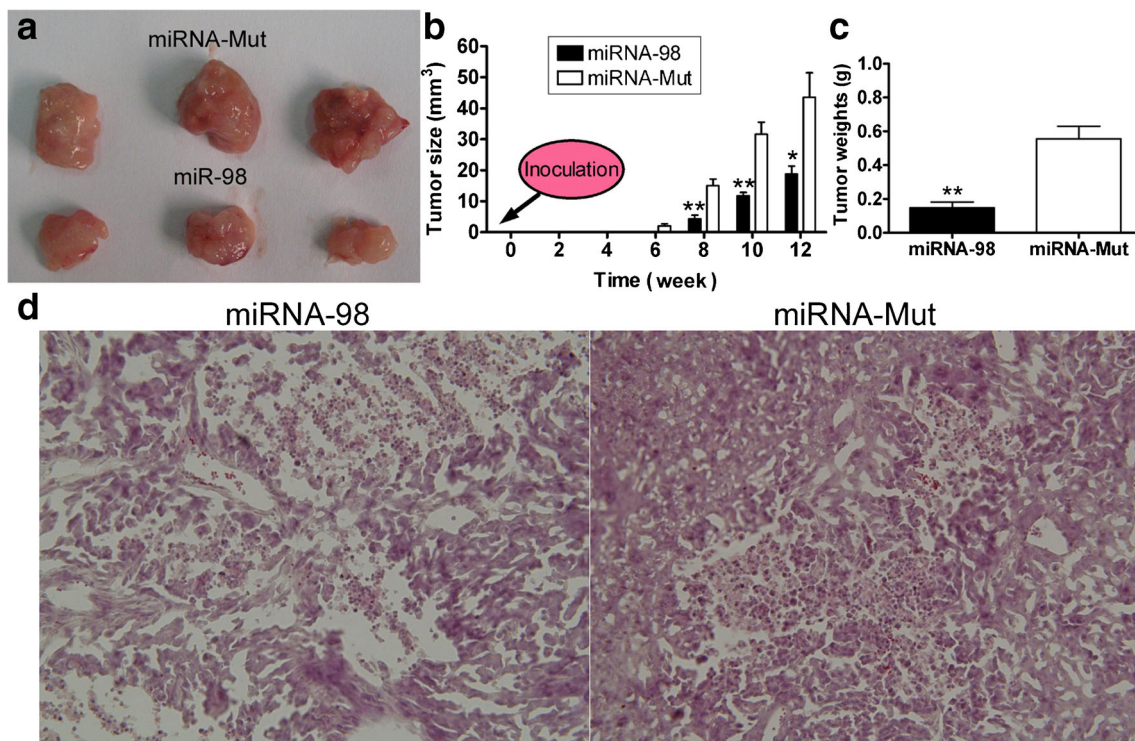


**Fig. 4** miRNA-98 inhibits the growth of OCSCs in vivo. **a** miRNA-98 or miRNA-Mut transfected human OCSCs were subcutaneously inoculated into SCID mice. Images of the excised xenograft tumors were shown here. **b** miRNA-98 expression delayed tumor growth. All mice in the miRNA-Mut transfected group developed tumors approximately 8 weeks after injection; tumors formed by the miRNA-98 transfected cells grew more slowly (\*\* $P < 0.01$  vs. miRNA-Mut; \* $P < 0.05$  vs. miRNA-Mut;  $n = 3$ ). **c** Tumor weight at 12 weeks (\*\* $P < 0.01$  vs. miRNA-Mut;  $n = 3$ ). **d**

Hematoxylin and eosin staining of tumor tissues formed in the miRNA-Mut transfected group and miRNA-98 transfected group revealing the cellular heterogeneity. Original magnification:  $\times 100$ . Representative H&E staining sections of all subcutaneous xenograft tumors derived from miRNA-98 transfected group or miRNA-Mut transfected OCSCs spheroid cells were categorized as serous adenocarcinomas of moderate/poor differentiation (Grade II/III), similar to the parental primary patient tumors

formed from miR-98 transfected cells grew more slowly than those formed from mutant miR-98 transfected cells (Fig. 4). Mice developed tumors approximately 12 weeks after inoculation with OCSCs transfected with mutant miR-98 from either cell line (Fig. 4). In contrast, only one of the three mice inoculated with miR-98 transfected OCSCs developed a tumor in the same time period. In addition, tumors obtained from the mutant miR-98-transfected group were significantly heavier than those from the miR-98 transfected group (Fig. 4). Representative hematoxylin and eosin (H&E)-stained sections of all subcutaneous xenograft tumors derived from both miR-98 or Mut-transfected OCSCs were categorized as serous ovarian cancer of moderate or poor differentiation (Fig. 4). In summary, xenografts formed by miR-98 transfected OCSCs were smaller, with reduced proliferation capacity than those formed by mutant miR-98 transfected OCSCs.

## Discussion

Current evidence suggests that the capacity for ovarian tumor formation and growth resides exclusively in a small proportion of tumor cells, termed OCSCs. OCSCs were first isolated from

human ovarian tumor tissue based on the specific expression of CD44/CD117 cell-surface antigens [2, 4]. The observation that stem cells and OCSCs share the common defining features of incomplete differentiation and a capacity for self-renewal and invasion have led to the cancer stem cell hypothesis, suggesting that the proliferation and invasion of a small subpopulation of cells is responsible for tumor growth [1, 2]. The OCSCs are known to possess an enhanced tumor-initiating capacity, with an ability of self-renewal, a low degree of differentiation, highly invasive, and generally more resistant than other cancer cells to conventional anticancer therapeutics [1–4]. These properties link OCSCs to tumor recurrence and distant metastasis; therefore, it is essential to elucidate their unique signaling and regulatory mechanisms in order to design specific therapies that target OCSCs. However, the mechanisms controlling OCIC proliferation is complicated and thus far poorly understood. To date, several reports indicate that EZH2 protein is overexpressed in some cancer cells [24–26].

To evaluate changes in the PcG family of proteins, and evaluate the potential for these changes to affect prostate carcinoma, cell cycle distribution and expression of Cdk proteins in a prostate cancer cell line expressing an EZH2-specific miRNA-98 were analyzed. qRT-PCR assays demonstrated



that levels of EZH2 mRNA were significantly reduced in miRNA-98 transfected OCSCs compared to miRNA-Mut transfected and untransfected cells 72 h after transfection. Subsequently, MTT assays and flow cytometry analysis detected an inhibition of proliferation and an arrest of cells in the G<sub>0</sub>/G<sub>1</sub> phase for miRNA-98 transfected OCSCs. To further identify the proteins involved in cell cycle regulation that are affected by EZH2, co-IP assays and Western blot analysis were performed. Cyclin E, p21, as well as the PcG-group family of proteins, HDAC1, pRb, E2F1, and c-Myc were detected. p21<sup>CIP1/WAF1</sup> was up-regulated, while the CDK2/Cyclin E complex and c-Myc were down-regulated. For the pRb-E2F pathway factors, E2F1, pRb, and HDAC, they had decreased expression in OCSCs transfected with miRNA-98.

Based on the results from this study, we propose a model (Fig. 3) of cell cycle regulation where the PcG-group protein, EZH2, signals through the CDK–pRb–E2F signaling pathway. This model is based on the experiments performed in this study that demonstrated the following points: (1) EZH2-targeted miRNA-98 decreased EZH2 expression and inhibited proliferation of the human OCSCs; (2) EZH2 affected the expression of the cell cyclin proteins p21, and cyclin E-CDK2 complex, as well as HDAC1, E2F1, and pRb. It is hypothesized that inhibition of EZH2 by miRNA-98 affected additional proteins than those specifically identified in this study, and therefore variances in the level of protein expression of p21, Cyclin E, c-Myc, HDAC1, E2F1, and pRb reflect the complex interplay of proteins that regulate the cell cycle of human OCSCs. Therefore, additional studies are needed to further elucidate the cell cycle signaling of prostate cancer cells; however, we have shown that EZH2 has an important role.

**Acknowledgments** This work was supported by grant from the National Natural Science Foundation of China (No. 81202811) and the Shanghai Municipal Health Bureau Fund (No. 20124320) to Te Liu.

**Conflicts of interest** None

## References

- Zhang S, Balch C, Chan MW, Lai HC, Matei D, Schilder JM. Identification and characterization of ovarian cancer-initiating cells from primary human tumors. *Cancer Res.* 2008;68:4311–20.
- Liu T, Cheng W, Lai D, Huang Y, Guo L. Characterization of primary ovarian cancer cells in different culture systems. *Oncol Rep.* 2010;23:1277–84.
- Qin W, Ren Q, Liu T, Huang Y, Wang J. MicroRNA-155 is a novel suppressor of ovarian cancer-initiating cells that targets CLDN1. *FEBS Lett.* 2014;587:1434–9.
- Cheng W, Liu T, Wan X, Gao Y, Wang H. MicroRNA-199a targets cd44 to suppress the tumorigenicity and multidrug resistance of ovarian cancer-initiating cells. *FEBS J.* 2012;279:2047–59.
- Sher F, Rossler R, Brouwer N, Balasubramaniyan V, Boddeke E, Copray S. Differentiation of neural stem cells into oligodendrocytes: involvement of the polycomb group protein ezh2. *Stem Cells.* 2008;26:2875–83.
- Azuara V, Perry P, Sauer S, Spivakov M, Jorgensen HF, John RM, et al. Chromatin signatures of pluripotent cell lines. *Nat Cell Biol.* 2006;8:532–8.
- Rajasekhar VK, Begemann M. Concise review: roles of polycomb group proteins in development and disease: a stem cell perspective. *Stem Cells.* 2007;25:2498–510.
- Saramaki OR, Tammela TL, Martikainen PM, Vessella RL, Visakorpi T. The gene for polycomb group protein enhancer of zeste homolog 2 (EZH2) is amplified in late-stage prostate cancer. *Gene Chromosome Cancer.* 2006;45:639–45.
- Sparmann A, van Lohuizen M. Polycomb silencers control cell fate, development and cancer. *Nat Rev Cancer.* 2006;6:846–56.
- Fujii S, Ochiai A. Enhancer of zeste homolog 2 downregulates e-cadherin by mediating histone H3 methylation in gastric cancer cells. *Cancer Sci.* 2008;99:738–46.
- Bryant RJ, Cross NA, Eaton CL, Hamdy FC, Cunliffe VT. EZH2 promotes proliferation and invasiveness of prostate cancer cells. *Prostate.* 2007;67:547–56.
- Otte AP, Kwaks TH. Gene repression by polycomb group protein complexes: a distinct complex for every occasion? *Curr Opin Genet Dev.* 2003;13:448–54.
- Kuzmichev A, Jenuwein T, Tempst P, Reinberg D. Different EZH2-containing complexes target methylation of histone H1 or nucleosomal histone h3. *Mol Cell.* 2004;14:183–93.
- Kuzmichev A, Margueron R, Vaquero A, Preissner TS, Scher M, Kirmizis A, et al. Composition and histone substrates of Polycomb repressive group complexes change during cellular differentiation. *Proc Natl Acad Sci U S A.* 2005;102:1859–64.
- Dykhoo DM, Palliser D, Lieberman J. The silent treatment: siRNAs as small molecule drugs. *Gene Ther.* 2006;13:541–52.
- Dykhoo DM, Lieberman J. The silent revolution: RNA interference as basic biology, research tool, and therapeutic. *Annu Rev Med.* 2005;56:401–23.
- Doench JG, Petersen CP, Sharp PA. siRNAs can function as miRNAs. *Genes Dev.* 2003;17:438–42.
- Fedorov Y, King A, Anderson E, Karpilow J, Ilsley D, Marshall W, et al. Different delivery methods—different expression profiles. *Nat Methods.* 2005;2:241.
- Heidel JD, Hu S, Liu XF, Triche TJ, Davis ME. Lack of interferon response in animals to naked siRNAs. *Nat Biotechnol.* 2004;22:1579–82.
- Xu F, Wang H, Zhang X, Liu T, Liu Z. Cell proliferation and invasion ability of human choriocarcinoma cells lessened due to inhibition of sox2 expression by microRNA-145. *Exp Ther Med.* 2012;5:77–84.
- Zhang L, Liu T, Huang Y, Liu J. MicroRNA-182 inhibits the proliferation and invasion of human lung adenocarcinoma cells through its effect on human cortical actin-associated protein. *Int J Mol Med.* 2011;28:381–8.
- Wu S, Huang S, Ding J, Zhao Y, Liang L, Liu T, et al. Multiple microRNAs modulate p21Cip1/Waf1 expression by directly targeting its 3' untranslated region. *Oncogene.* 2010;29:2302–8.
- Jansson MD, Lund AH. microRNA and cancer. *Mol Oncol.* 2012;6:590–610.
- Richter GH, Plehm S, Fasan A, Rossler S, Unland R, Bennani-Baiti IM, et al. EZH2 is a mediator of EWS/FL1 driven tumor growth and metastasis blocking endothelial and neuro-ectodermal differentiation. *Proc Natl Acad Sci U S A.* 2009;106:5324–9.
- Simon JA, Lange CA. Roles of the EZH2 histone methyltransferase in cancer epigenetics. *Mutat Res.* 2008;647:21–9.
- Bachmann IM, Halvorsen OJ, Collett K, Stefansson IM, Straume O, Haukaas SA, et al. EZH2 expression is associated with high proliferation rate and aggressive tumor subgroups in cutaneous melanoma and cancers of the endometrium, prostate, and breast. *J Clin Oncol.* 2006;24:268–73.